doi:10.1093/brain/aws313 Brain 2013: 136; 116–131 | 116

BRAIN
A JOURNAL OF NEUROLOGY

Fibronectin aggregation in multiple sclerosis lesions impairs remyelination

Josephine M. J. Stoffels,[1] Jenny C. de Jonge,[1] Mirjana Stancic,[1] Anita Nomden,[1] Miriam E. van Strien,[2] Dan Ma,[3] Zuzana Šišková,[1] Olaf Maier,[1] Charles ffrench-Constant,[4] Robin J. M. Franklin,[3] Dick Hoekstra,[1] Chao Zhao[3] and Wia Baron[1]

1 Department of Cell Biology, University Medical Centre Groningen, University of Groningen, 9713 AV Groningen, The Netherlands
2 Department of Anatomy and Neurosciences, Neuroscience Campus Amsterdam, VU University Medical Centre, 1007 MB Amsterdam, The Netherlands
3 Wellcome Trust - Medical Research Council Stem Cell Institute and Department of Veterinary Medicine, University of Cambridge, Madingley Road, Cambridge CB3 0ES, UK
4 MRC Centre for Regenerative Medicine, Centre for Multiple Sclerosis Research, Edinburgh, EH16 4UU, UK

Correspondence to: Wia Baron, Department of Cell Biology,
University Medical Centre Groningen,
University of Groningen,
A. Deusinglaan 1,
9713 AV Groningen,
The Netherlands
E-mail: w.baron@umcg.nl

Correspondence may also be addressed to: Chao Zhao, Wellcome Trust - Medical Research Council Stem Cell Institute and Department of Veterinary Medicine, University of Cambridge, Madingley Road, Cambridge CB3 0ES, UK. E-mail: cz213@cam.ac.uk

Remyelination following central nervous system demyelination is essential to prevent axon degeneration. However, remyelination ultimately fails in demyelinating diseases such as multiple sclerosis. This failure of remyelination is likely mediated by many factors, including changes in the extracellular signalling environment. Here, we examined the expression of the extracellular matrix molecule fibronectin on demyelinating injury and how this affects remyelination by oligodendrocytes progenitors. In toxin-induced lesions undergoing efficient remyelination, fibronectin expression was transiently increased within demyelinated areas and declined as remyelination proceeded. Fibronectin levels increased both by leakage from the blood circulation and by production from central nervous system resident cells. In chronically demyelinated multiple sclerosis lesions, fibronectin expression persisted in the form of aggregates, which may render fibronectin resistant to degradation. Aggregation of fibronectin was similarly observed at the relapse phase of chronic experimental autoimmune encephalitis, but not on toxin-induced demyelination, suggesting that fibronectin aggregation is mediated by inflammation-induced demyelination. Indeed, the inflammatory mediator lipopolysaccharide induced fibronectin aggregation by astrocytes. Most intriguingly, injection of astrocyte-derived fibronectin aggregates in toxin-induced demyelinated lesions inhibited oligodendrocyte differentiation and remyelination, and fibronectin aggregates are barely expressed in remyelinated multiple sclerosis lesions. Therefore, these findings suggest that fibronectin aggregates within multiple sclerosis lesions contribute to remyelination failure. Hence, the inhibitory signals induced by fibronectin aggregates or factors that affect fibronectin aggregation could be potential therapeutic targets for promoting remyelination.

Keywords: fibronectin; multiple sclerosis; remyelination; astrocyte; oligodendrocyte

Received April 28, 2012. Revised September 9, 2012. Accepted October 1, 2012

Abbreviations: EAE = experimental autoimmune encephalomyelitis; MBP = myelin basic protein; MTT = 3-(4,5-Dimethylthiazol-2-yl)-2,5-diphenyltetrazolium bromide; GFAP = glial fibrillary acidic protein; PBS = phosphate buffered saline.

Introduction

Inflammation-mediated loss of myelin (demyelination) and incomplete remyelination are pathological hallmarks of multiple sclerosis. Remyelination is essential for both restoration of saltatory conduction and axonal protection (Franklin and ffrench-Constant, 2008). Although remyelination occurs in early stages of multiple sclerosis, it declines as the disease progresses, resulting in chronically demyelinated plaques and axonal loss (Goldschmidt *et al*., 2009). Oligodendrocyte progenitors, the cells responsible for CNS remyelination (Zawadzka *et al*., 2010), are present in most multiple sclerosis lesions, but ultimately fail to differentiate into mature myelinating oligodendrocytes, which results in remyelination failure (Franklin and ffrench-Constant, 2008; Kuhlmann *et al*., 2008).

Migration and proliferation of oligodendrocyte progenitor cells and their differentiation into myelinating oligodendrocytes are regulated by many factors, including the extracellular matrix (Baron *et al*., 2005). For example, laminin-2 provides oligodendrocytes with signals for both survival (Colognato *et al*., 2002; Baron *et al*., 2003) and myelination (Buttery and ffrench-Constant, 1999; Relvas *et al*., 2001; Siskova *et al*., 2006). In contrast, fibronectin promotes proliferation, but reduces myelin-like membrane formation (Buttery and ffrench-Constant, 1999; Baron *et al*., 2005; Maier *et al*., 2005; Siskova *et al*., 2006, 2009). Following CNS injury, the extracellular matrix is extensively remodelled, which is reflected in altered expression profiles of extracellular matrix molecules (Sobel and Mitchell, 1989; Gutowski *et al*., 1999; Back *et al*., 2005; van Horssen *et al*., 2005, 2006; Satoh *et al*, 2009). Therefore, aberrant extracellular matrix signals in the injury environment may inhibit oligodendrocyte maturation, contributing to remyelination failure in multiple sclerosis lesions. Indeed, while absent from healthy adult human tissue, expression of fibronectin is upregulated in multiple sclerosis lesions, particularly around blood vessels (Sobel and Mitchell, 1989; van Horssen *et al*., 2005), and also in the CNS parenchyma (van Horssen *et al*., 2006). Furthermore, astrocyte-derived high molecular weight hyaluronan, which inhibits oligodendrocyte maturation, appears in chronic demyelinating multiple sclerosis lesions (Back *et al*., 2005). Laminin expression is also increased in multiple sclerosis lesions (van Horssen *et al*., 2005). Therefore, the overall effects of lesion-induced changes in the extracellular matrix on oligodendrocyte progenitor cells remain to be established.

Here, we further characterized the nature of fibronectin signalling to oligodendrocyte progenitor cells in multiple sclerosis lesions, and how this fibronectin signalling might affect remyelination. We show that fibronectin specifically localizes in areas of demyelination, and identify cellular sources for its expression. In experimental demyelination, fibronectin is cleared on remyelination, whereas fibronectin aggregates and therefore persists in chronic multiple sclerosis lesions and chronic relapsing experimental autoimmune encephalomyelitis (EAE). Importantly, intralesion injection of fibronectin aggregates inhibits oligodendrocyte differentiation and remyelination in toxin-induced demyelinated lesions, which implies that aggregation of fibronectin contributes to remyelination failure in multiple sclerosis lesions.

Materials and methods

Multiple sclerosis lesions

Tissues were obtained from the Netherlands Brain Bank, Netherlands Institute for Neuroscience, Amsterdam. Studies were performed on brain material taken at autopsy from nine healthy subjects (without clinical or histological signs of neurological disease), eight subjects with (chronic) active multiple sclerosis lesions, nine with chronic inactive multiple sclerosis lesions and two with multiple sclerosis shadow plaques (Maier *et al*., 2007). Samples were selected according to their activity status as determined by MRI, split in half and either immediately frozen in liquid nitrogen or fixed in formaldehyde and paraffin embedded. Control white matter did not show any histological signs of inflammation and demyelination. Demyelinated lesions were identified by Luxol fast blue histochemistry and proteolipid protein staining. Active lesions were characterized by their indistinct margin, hypercellularity, intense perivascular T lymphocyte infiltration (CD3) and presence of hypertrophic astrocytes (glial fibrillary acidic protein, GFAP) and macrophages (CD68) in the centre of the lesions. Chronic active lesions were classified on the basis of a hypocellular lesion centre with fibrous astrocytes and some macrophages, sharp lesion border and a broad rim of macrophages. Chronic inactive lesions contained a hypocellular centre without macrophages and lymphocytes, and a sharp lesion border. Shadow plaques were characterized by a slightly reduced proteolipid protein expression compared with the surrounding normal-appearing white matter, without abundant expression of CD68. Notably, remyelinated areas, as determined by Luxol fast blue or proteolipid protein staining, were not visible in the other multiple sclerosis lesions analysed. For immunohistochemical analysis, sections were deparaffinized and subjected to antigen retrieval followed by fluorescent detection as described previously (Stancic *et al*., 2011). Control sections from which the primary antibody was omitted showed low non-specific binding. Sections were analysed using a conventional fluorescence microscope (Olympus AX70) equipped with analySIS software. For western blot and reverse transcription–PCR analysis, samples were homogenized and extracted for protein and total RNA as described (Maier *et al*., 2007). All material was collected from donors whose written informed consent for brain autopsy and the use of the material and clinical information for research purposes has been obtained by the Netherlands Brain Bank.

Toxin-induced demyelination

Lesions were induced in spinal cord white matter or in the caudal cerebral peduncle of 8–10-week-old female Sprague Dawley rats

(Harlan) by injection of 1 µl of 1% lysolecthin (Sigma Aldrich) or 4 µl of 0.01% ethidium bromide (VWR), respectively (Fancy *et al*., 2004; Zhao *et al*., 2006). At the desired time points, animals were sacrificed and tissue processed as described previously (Woodruff and Franklin, 1999; Fancy *et al*., 2004; Zhao *et al*., 2006). The control spinal cord tissues consisted of similar fragments from unlesioned thoracic segments of spinal cord. The intralesion injection of fibronectin aggregates was performed at 7 days post lesion into lysolecithin-induced lesions in rat dorsal funiculus of spinal cord. A volume of 2 µl of fibronectin aggregates (0.3 µg/µl) was injected using a Hamilton syringe with a pulled glass tip attached. These animals were sacrificed 7 days after aggregate injection, i.e. 14 days post lesion. Experiments were performed in compliance with UK Home Office regulations.

Chronic relapsing experimental autoimmune encephalomyelitis

Chronic relapsing EAE was induced with recombinant rat myelin oligodendrocyte glycoprotein in adult male Dark Agouti rats (Harlan, weight 230–250 g) as described previously (Ledeboer, *et al*., 2003). Briefly, the rats were anaesthetized with isoflurane and immunized intradermally in the dorsal tail base with 75 µg of recombinant rat myelin oligodendrocyte glycoprotein ($rrMOG_{1-125}$) emulsified in incomplete Freund's adjuvant (Difco) together with 10 mM NaAc (pH 3.0). Control rats received incomplete Freund's adjuvant and NaAc only. Rats were weighed and examined daily for neurological symptoms of EAE that were scored on the following scale: 0, no clinical disease; 0.5, partial loss of tail tone; 1, complete tail atony; 2, paresis, partial hind limb paralysis; 3, complete paralysis of the hind limbs and/or lower part of the body; 4, moribund or dead due to EAE. Chronic relapsing EAE and incomplete Freund's adjuvant control animals were sacrificed when chronic relapsing EAE rats reached the peak clinical symptoms during the relapse (~25 days post injection) and spinal cords were processed as previously described (Ledeboer *et al*., 2003; Maier *et al*., 2005). All experimental procedures were approved of by the Animal Ethical Committee of the VU University.

Cell cultures

Primary glial cells

Primary glial cultures were generated from 1 to 3-day-old Wistar rats (Harlan) as described previously (Bsibsi *et al*., 2012). Isolated microglia and astrocytes were cultured in Dulbecco's modified Eagle medium/10% foetal calf serum in 10 cm dishes (1.0×10^6/dish) or 8-well Permanox chamber slides (15 000 cells/well; Nunc). Cells were left untreated or activated with 200 ng/ml ultrapure lipopolysaccharide (InvivoGen) for 48 h. Deposited astroglial matrices were prepared by water-lysis of astrocytes for 2 h at 37°C. Isolated oligodendrocyte progenitor cells were cultured in Sato medium (Maier *et al*., 2005) in poly-L-lysine-coated 10 cm dishes (1.0×10^6/dish) or 8-well chamber slides (15 000 cells/well) with wells coated with astroglial matrices (see later in the text). The oligodendrocyte progenitor cells were first synchronized in Sato medium supplemented with platelet-derived growth factor AA (Peprotech; 10 ng/ml) and fibroblast growth factor-2 (Peprotech, 10 ng/ml) for 2 days. Differentiation was induced by growth factor withdrawal and cells were grown for 7 days in Sato medium containing 0.5% foetal calf serum.

Human astrocytes

Adult human astrocytes were isolated from post-mortem subcortical white matter of well-documented healthy subjects and patients with multiple sclerosis, as described previously (Bsibsi *et al*., 2002). Purity of the cultures was routinely verified by staining for GFAP (astrocytes). Astrocyte cultures used were at least 97% pure. The cells were plated in 10 cm dishes (1.0×10^6/dish) or 8-well chamber slides (10 000/well). Deposited astroglial matrices were prepared by water-lysis of astrocytes for 2 h at 37°C.

Immunohistochemical analysis

Toxin-induced lesions

Frozen sections (12 µm) of spinal cord and caudal cerebral peduncle were permeabilized and blocked with phosphate-buffered saline (PBS) containing 5% normal donkey serum and 0.3% Triton™ X-100. Sections were incubated with the appropriate primary antibodies (Table 1) diluted in PBS containing 3% normal donkey serum overnight at 4°C. For double labelling immunohistochemistry, primary antibodies were incubated sequentially. After washing in PBS, the sections were incubated with appropriate Alexa Fluor® (488 or 594)-conjugated secondary antibodies (Invitrogen 1:500) at room temperature for 2 h, followed by 4′,6-diamidino-2-phenylindole (DAPI) to visualize cell nuclei. Following immunostaining, some slides were incubated in 0.1% Sudan Black solution (made in 70% ethanol) for 5 min at room temperature to stain myelin. Pale areas in the white matter indicate loss of myelin. Sudan Black staining has no detrimental effect

Table 1 Primary antibodies used during immunohistochemistry, immunocytochemistry and western blot

Antibody	Manufacturer	Dilution western blot	Dilution IHC/ICC
Anti-actin (mAb)	Sigma	1:1000	n.a.
Anti-APC (CC1, mAb)	Calbiochem	n.a.	1:200
Anti-CD3 (mAb)	Zymed	n.a.	1:100
Anti-CD11b (MAC1, mAb)	Serotec	n.a.	1:100
Anti-CD68 (mAb)	DAKO	n.a.	1:100
Anti-CNP (mAb)	Sigma	1:500	n.a.
Anti-EIIIA-fibronectin (IST9)	Abcam	n.a.	1:200
Anti-fibronectin (pAb)	Millipore	1:1000	1:50–1:100
Anti-GFAP (mAb)	Millipore	1:1000	1:500
Anti-GFAP (pAb)	DAKO	n.a.	1:500
Anti-laminin 1 + 2 (pAb)	Abcam	1:500	n.a.
Anti-MBP (mAb)	Chemicon	1:100	1:25
Anti-Nkx2.2 (mAb)	Hybridoma Bank Iowa	n.a.	1:100
Anti-Olig2 (pAb)	Millipore	n.a.	1:1000
Anti-OX6 (mAb)	Serotec	n.a.	1:1000
Anti-PLP (mAb)	Serotec	n.a.	1:3000
TuJ1 (mAb)	kind gift of A. Frankfurter[a]	1:2000	n.a.
Anti-vWF (mAb)	Serotec	n.a.	1:50
Anti-vWF (pAb)	DAKO	n.a.	1:200

n.a. = not applicable; mAb = monoclonal antibody; pAb = polyclonal antibody; IHC/ICC = immunohistochemistry/immunocytochemistry.
a Lee *et al*., 1999.

Table 2 Primer sequences used during RT-PCR

Target	Sense	Anti-sense	Length (bp)
Actin Hs/Rn	ACCACACAGCTGAGAGGGAAATC	GGTCTTTACGGATGTCAACG	276
CD68 Hs	TATTGCTTTCTGCATCATCC	TTTAGTAGAGACAGGGTTTCAC	303
Cyclophilin Rn	CTCGTGACCCCTCTTTCC	CAT TATTTTCCTCATTTCCCCT	522
Fn1 Hs	GAGGAGAGTGGAAGTGTGAG	TTGTGGTTGTTGTATAGGAAGG	496
Fn1 Rn	AGCCC TTACAGTTCCAAGTTCC	CCATT CAATTCATTGCATCG	1077
GFAP Hs	CTCCAACTAACAAGAAACTCAC	GGCTCCAATCTATAATCCCA	412

Hs = *Homo sapiens*; Rn = *Rattus norvegicus*.

to immunofluorescence. Sections were analysed with a Zeiss Axio Observer A1 fluorescent microscope.

Chronic relapsing experimental autoimmune encephalomyelitis

Fresh frozen rat spinal cord sections (12 μm) were fixed with acetone for 20 min, washed in Tris-buffered saline, blocked in 5% milk in Tris-buffered saline with 0.5% Triton™ X-100 and 0.03% H_2O_2 and incubated with primary antibodies (Table 1) overnight at 4°C, followed by appropriate Alexa Fluor® (488 or 594)-conjugated secondary antibodies (1:400) for immunofluorescence. Sections were examined with a Leica confocal laser scanning microscope. For peroxidase-based analysis, sections were washed in Tris-buffered saline and incubated for 2 h at room temperature with secondary biotinylated IgGs (Jackson ImmunoResearch, 1:400), followed by washes in Tris-buffered saline and incubation for 1 h at room temperature with avidin–biotin–peroxidase complex (Vector Laboratories, 1:400). After washes in Tris-buffered saline and 50 mM Tris–HCl (pH 7.6), immunoreactivity was visualized using 0.5 mg/ml of diaminobenzidene (Sigma) in 50 mM Tris–HCl (pH 7.6).

Immunocytochemical analysis

Oligodendrocytes were fixed with 4% paraformaldehyde for 20 min and permeabilized with ice-cold methanol for 10 min. After a 30-min block with 4% bovine serum albumin, cells were incubated for 60 min with primary antibodies (Table 1) in 4% bovine serum albumin. Cells were washed three times with ice-cold PBS and incubated for 25 min with appropriate tetramethyl rhodamine iso-thiocyanate-conjugated antibodies (Jackson ImmunoResearch). Nuclei were stained with DAPI (1 μg/ml) and 1,4-diazabicyclo[2.2.2]octane-containing mounting medium was added to prevent image fading. For staining of astroglial matrices, fixation and permeabilization steps were omitted. Oligodendrocytes were characterized by their morphology, and in each experiment at least 500 cells were scored as myelin basic protein (MBP)-positive or -negative. In addition, positive cells bearing MBP-positive membranous structures spread between the cellular processes were identified as membrane sheet forming, irrespective of the extent of sheet formation.

Reverse transcription–polymerase chain reaction

Total RNA was isolated from cells and tissue homogenates using the RNeasy® Mini kit (Qiagen). Total RNA from tissue (0.5 μg) or cells (1.0 μg) was reverse transcribed in the presence of oligo(dT)12–18 and dNTPs (Invitrogen) with SuperScript® II reverse transcriptase (Invitrogen) according to the manufacturer's instructions. The resulting complementary DNA was amplified using primers specific to the different proteins (Table 2). Cycling conditions were optimized and PCR products were resolved by agarose gel electrophoresis. Changes in gene expression were analysed by Scion Image Software.

In situ hybridization

To generate a complementary RNA probe for fibronectin, complementary DNA acquired using fibronectin primers (Table 2) was cloned by reverse transcription–PCR and inserted into the pCRII-TOPO plasmid, using the TOPO® TA Cloning® Kit (Invitrogen) according to the manufacturer's instruction. The probe is expected to recognize all variants of fibronectin messenger RNA. The digoxigenin-labelled proteolipid protein probe was generated as described (Chari *et al*., 2006). The details for probe labelling and staining procedures have been described in previous studies (Sim *et al*., 2000; Zhao *et al*., 2008).

Deoxycholate (in)solubility assays and preparation of fibronectin aggregates

Tissue homogenates (multiple sclerosis and chronic relapsing EAE) were incubated with deoxycholate buffer [2% deoxycholate and Complete Mini protease inhibitor cocktail (Roche) in 20 mM Tris–HCl, pH 8.3], for 30 min on ice. Proteins from lysolecithin-induced lesions were extracted from 30-μm thick slices through oscillation for at least 3 h in deoxycholate buffer. Deposited astroglial matrices were prepared by water-lysis of astrocytes for 2 h at 37°C. The efficiency of lysis was verified by DAPI staining, and only matrices without visible nuclei were used. Deposits were scraped in ice-cold deoxycholate buffer and further solubilized for 30 min on ice. Protein concentrations were determined by a Bio-Rad DC protein assay (Bio-Rad Laboratories) using bovine serum albumin as standard. For biochemical analysis, deoxycholate-soluble and -insoluble fractions from equal protein amounts of the deoxycholate extracts were separated by centrifugation at 13 000 rpm for 20 min at 4°C. The deoxycholate-insoluble pellets were dissolved in 2% SDS in 20 mM Tris–HCl, pH 8.8, whereas the deoxycholate-soluble supernatant was concentrated by trichloroacetic acid precipitation. For intralesion injections, the aggregates present in the deoxycholate-insoluble fraction were dialyzed against PBS for 24 h at 4°C. After dialysis, the protein content was determined and the presence of aggregates confirmed by western blot.

Lactate dehydrogenase and MTT assay

Oligodendrocyte progenitor cells were plated in 24-well plates (Nunc) at a density of 50 000 cells in 500 μl culture medium.

Oligodendrocytes were treated with fibronectin aggregates (5.0 μg/ml of the deoxycholate-insoluble fraction of rat astrocyte-derived deposits dialyzed against PBS) at the onset of differentiation (oligodendrocyte progenitor cells), 3 days (immature oligodendrocytes) or 7 days (mature oligodendrocytes) after initiating differentiation. After 3 days, the medium (lactate dehydrogenase assay) and cells [3-(4,5-Dimethylthiazol-2-yl)-2,5-diphenyltetrazolium bromide; MTT] were analysed. To determine the cytotoxicity of deoxycholate-insoluble fibronectin aggregates, the release of lactate dehydrogenase into the medium was measured using a commercial lactate dehydrogenase assay kit (Roche) according to manufacturer's instructions. The effect on cell viability was determined with an MTT assay. Briefly, after medium was removed for the lactate dehydrogenase assay, cells were incubated with MTT diluted in culture medium (0.5 mg/ml, Sigma) for 3–4 h. MTT-formazan crystals were collected in dimethyl sulphoxide and absorption was measured at 560 nm. Cytotoxicity (lactate dehydrogenase) and cell viability (MTT) are expressed as the percentage of vehicle-treated (PBS) cells, which was set at 100%.

Electron microscopy analysis

The animals were perfused with 4% glutaraldehyde and lesion containing spinal cord was coronally sliced at ~1 mm thickness and fixed with osmium tetroxide overnight before being subjected to a standard protocol of epoxy resin embedding (Zhao *et al*., 2008). Ultrathin sections of the lesion site were produced at transverse orientation and examined with a Hitachi H-600 electron microscope. Myelination of axons in the lesion was analysed for g-ratio, which is calculated as the diameter of axons divided by the diameter of axons with surrounding myelin sheaths.

Sodium dodecyl sulphate–polyacrylamide gel electrophoresis and western blotting

Equal amounts of proteins (tissue homogenates, cultured cells and reducing conditions) or volume [deoxycholate-(in)solubility assays, non-reducing conditions] were loaded onto 6 or 8% SDS-PAGE gels and subjected to western blot analysis as described previously (Bsibsi *et al*., 2012). The signals were detected using the Odyssey® Infrared Imaging System (Li-Cor Biosciences) and analysed using Odyssey V3.0 analysis software.

Results

Cellular fibronectin expression is transiently increased in toxin-induced demyelination

Fibronectin effects on regeneration have been studied in various tissues (Scanzello *et al*., 2008). To assess whether on demyelination, changes in the extracellular matrix environment include fibronectin, we first examined the profile of fibronectin expression following toxin-induced demyelination. Injection of lysolecithin into spinal cord white matter creates focally demyelinated lesions without significant axonal loss (Blakemore and Franklin, 2008). These lesions undergo spontaneous remyelination, involving the activation of oligodendrocyte progenitor cells and their recruitment into the demyelinated area (0–10 days post lesion), and their subsequent differentiation and myelin sheath formation (10–21 days post lesion) (Zhao *et al*., 2006). In this model, the lesion area is characterized by an increased cellularity, which reflects well the area of demyelination as visualized with a Sudan Black myelin stain (Fig. 1A). Therefore, the demyelinated areas were identified based on their hypercellularity using DAPI staining for nuclei. Immunohistochemical analysis showed that fibronectin expression was highly detectable in demyelinated areas at 3 and 5 days post lesion, but progressively reduced at 10 and 15 days post lesion (Fig. 1B). Western blot analysis confirmed a clear and significant increase in fibronectin protein expression at 5 days post lesion, followed by a significant decrease at 14 days post lesion (Fig. 1C). Demyelination and ongoing remyelination of the lesions were confirmed by reduced expression levels of MBP at 5 days post lesion compared with unlesioned control, and increased MBP expression at 14 days post lesion as compared with 5 days post lesion, respectively (Fig. 1C). Transient expression of fibronectin was also observed using a second model of toxin-induced demyelination, in which ethidium bromide is injected into the caudal cerebral peduncle of rats (Supplementary Fig. 1; Woodruff and Franklin, 1999).

Fibronectin has two major variants: (i) plasma fibronectin, a soluble dimer that is secreted into the circulation by hepatocytes; and (ii) cellular fibronectin, which is produced by resident cells. On CNS injury, and likely also on toxin-induced demyelination, plasma fibronectin enters the brain owing to blood–brain barrier disruption (Sobel and Mitchell, 1989; van Horssen *et al*., 2005). To examine whether cells also express cellular fibronectin following CNS demyelination, we analysed fibronectin messenger RNA expression in lysolecithin-induced demyelination via reverse transcriptase–PCR. As shown in Fig. 1D, total fibronectin messenger RNA levels increased significantly at demyelination (5 days post lesion) compared with unlesioned spinal cord, and decreased again in early remyelination (14 days post lesion). To assess cellular fibronectin protein expression, we performed double immunohistochemistry with anti-fibronectin and anti-EIIIA (IST9) specific antibodies. EIIIA-fibronectin, i.e. cellular fibronectin, was expressed in acute lysolecithin-induced demyelination, where it was confined to the lesioned area and mostly located around blood vessels (Fig. 1E). Notably, fibronectin expression was more widespread throughout the demyelinated area than EIIIA-fibronectin. Importantly, EIIIA-fibronectin protein expression was increased as early as 1 day post lesion and downregulated at 14 days post lesion (Supplementary Fig. 2), concomitant to the decrease of total fibronectin expression (Fig. 1B and C). Hence, these findings reveal that fibronectin expression was transiently upregulated on toxin-induced demyelination, and the detection of fibronectin messenger RNA and EIIIA-fibronectin indicate that CNS resident cells synthesize fibronectin in response to demyelination, which prompted us to identify these cells.

Multiple cell types express cellular fibronectin in toxin-induced demyelination

The cellular distribution of fibronectin messenger RNA in toxin-induced demyelination sections was examined by *in situ*

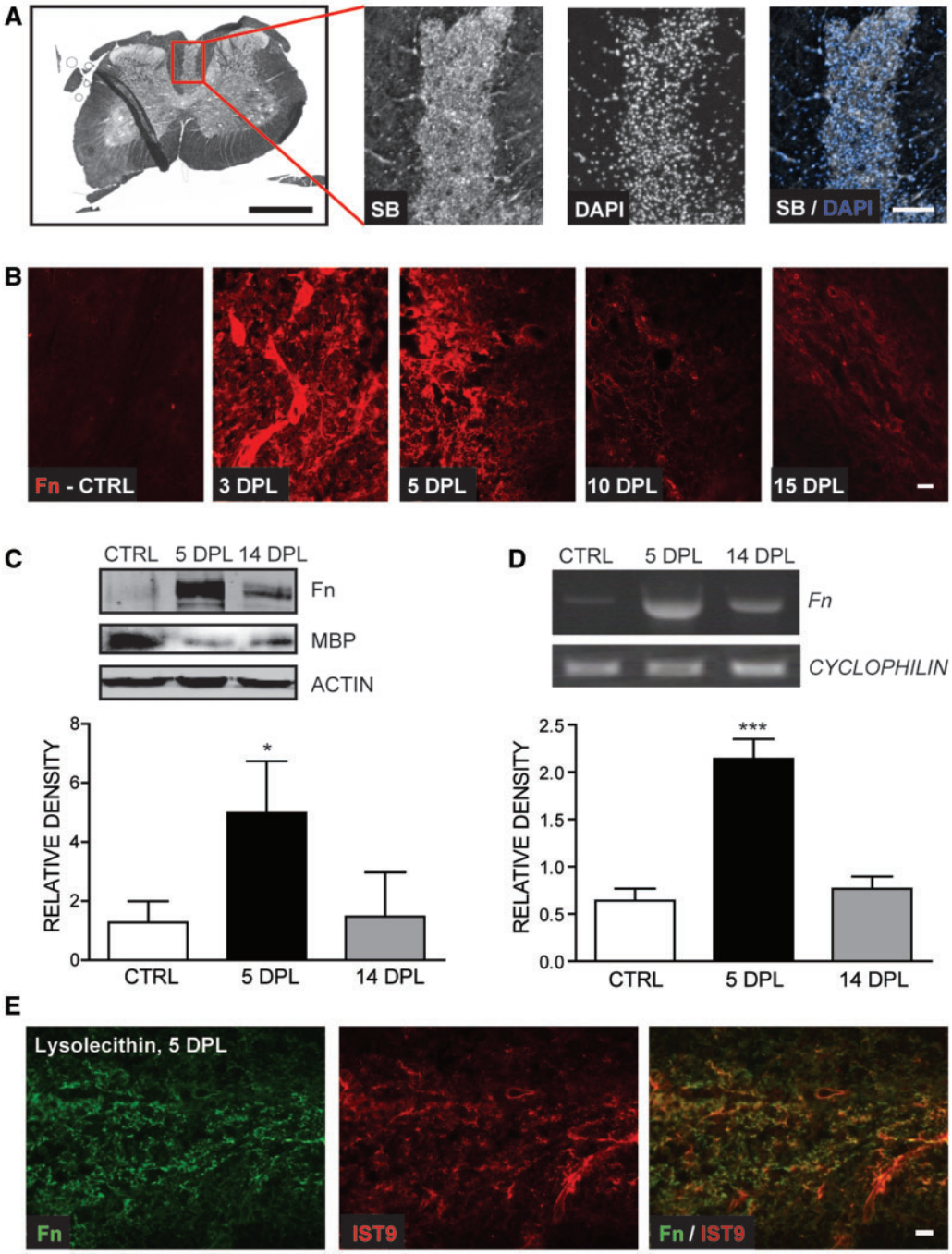

Figure 1 Expression of cellular fibronectin in lysolecithin-induced demyelination. Lesioned and non-lesioned tissue were analysed for the expression of fibronectin protein and messenger RNA using fluorescent immunohistochemistry (**B** and **E**), western blot (**C**) and reverse transcriptase–PCR (**D**) analysis. Focal demyelination of the rat spinal cord was induced by lysolecithin injection. In **A–E**, representative images, blots and gels are shown of three to four animals per condition. (**A**) Demyelinated areas, as visualized with a Sudan Black (SB) myelin stain, were identified based on their hypercellularity (DAPI staining). Images were taken at 5 days post lesion. Scale bars are 1000 μm (black) and 100 μm (white). (**B**) Fibronectin expression (red) is abundant at demyelination (3 and 5 days post lesion), and cleared on remyelination (10 and 15 days post lesion). The baseline expression of fibronectin was low on immunostaining of unlesioned control spinal cord and normal-appearing tissue around lesions (CTRL). Scale bar = 20 μm. (**C** and **D**) Fibronectin protein (**C**) and messenger RNA (**D**) is upregulated in demyelination [5 days post lesion versus control (CTRL)], but downregulated on remyelination (14 days post lesion versus 5 days post lesion). Data were quantified by normalizing the optical densities of fibronectin protein against actin (**C**), and fibronectin messenger RNA against the housekeeping gene cyclophilin (**D**). Data are expressed as value of the mean + the standard deviation (SD) ($*P < 0.05$, $***P < 0.0001$ at one-way ANOVA followed by Tukey's honestly significant difference test, three to four animals per condition). Demyelination of the lesions was confirmed by lower expression levels of the myelin protein MBP. (**E**) Fibronectin (red) and EIIIA-fibronectin (IST9, green) expression in lysolecithin-induced demyelination (5 days post lesion). Scale bar = 20 μm. EIIIA-fibronectin and fibronectin particularly co-localize (yellow) around blood vessels. Fn = fibronectin; DPL = days post lesion.

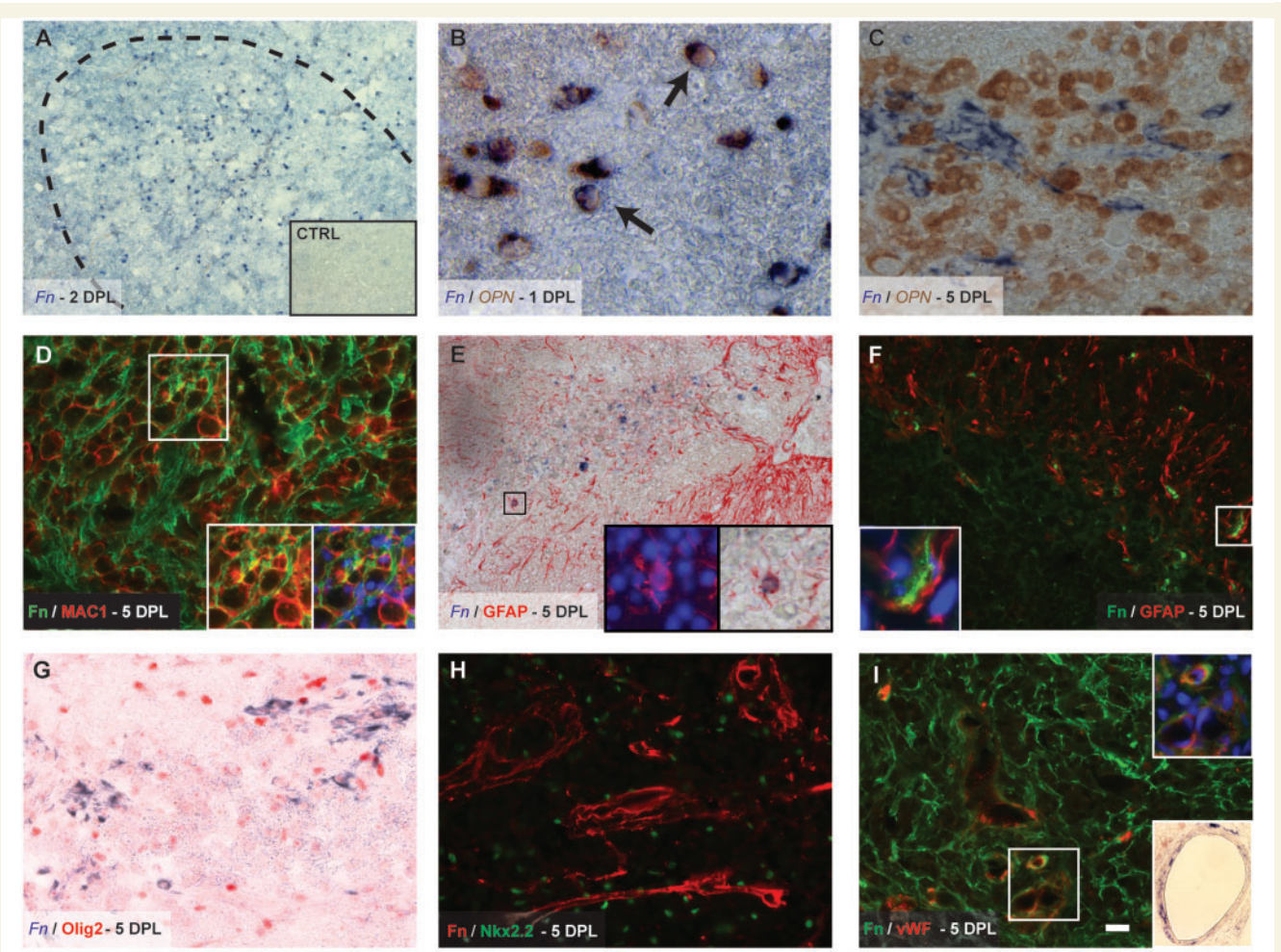

Figure 2 Expression of fibronectin by a variety of cell types in toxin-induced demyelination. Fibronectin messenger RNA in lesioned areas is expressed in microglia/macrophages (**B**), astrocytes (**E**) and endothelial cells (inset **I**), but not oligodendrocytes (**G**). Sections from non-lesioned (inset **A**), caudal cerebral peduncle lesions (**A**, **E** and **F**) and spinal cord lesions (lysolecithin, **B–D** and **G–I**) at 1 day post lesion (**B**), 2 days post lesion (**A**) and 5 days post lesion (**C–I**) were single (**A**, inset **A** and **I**) or double (**B–I**) labelled for either fibronectin protein (green, **D**, **F**, **I** and red, **H**) or fibronectin messenger RNA (**A–C**, **E**, **G**, inset **I**, blue) together with osteopontin (OPN) messenger RNA (**B** and **C**, magenta) and MAC1 (**D**, red) as markers for microglia/macrophages, GFAP (**D** and **E**, red), as a marker for astrocytes, Olig2 (**G**, red) as a marker for the oligodendrocyte lineage, Nkx2.2 (**H**, green) as a marker for oligodendrocyte progenitor cells, and Von Willebrand factor (vWF, **I**, red), as a marker for endothelial cells. Protein and messenger RNA were visualized by indirect fluorescent immunohistochemistry and *in situ* hybridization, respectively. Lesioned areas were identified by hypercellularity, i.e. DAPI (blue) staining. Representative images of three to four animals per condition are shown. Scale bar = 50 μm for **A**, **E** and **H**, and 20 μm for **B–D**, **F**, **G** and **I**. Fn = fibronectin; DPL = day(s) post lesion.

hybridization. Fibronectin messenger RNA expression was confined to the demyelinated area (Fig. 2A), consistent with fibronectin protein expression (Fig. 1A). Macrophages/microglia were identified as a possible source by two-colour double labelling *in situ* hybridization for fibronectin and osteopontin messenger RNA, a marker for cells of the macrophage/microglia lineage particularly in toxin-induced lesions (Zhao *et al*., 2008). There was clear colocalization at 1 day post lesion (Fig. 2B; 68.2 ± 11.2%) that was decreased at 5 days post lesion (Fig. 2C; 23 ± 5.8%), which might reflect the transition from monocytes/microglia to phagocytotic macrophages (Zhao *et al*., 2006). This is supported by double labelling with anti-fibronectin and anti-CD11b (MAC1) antibodies, showing fibronectin expression in a substantial number of MAC1-positive microglia/macrophages (Fig. 2D, 5 days post lesion). Fibronectin messenger RNA (Fig. 2E) and protein (Fig. 2F) was further detected in GFAP-positive astrocytes, indicating that astrocytes are another source of cellular fibronectin. Co-labelling with anti-Olig2 antibodies (Fig. 2G; 2.9 ± 1.0% fibronectin messenger RNA/Olig2 double positive), as a marker for the oligodendrocytes lineage and antibodies against Nkx2.2 (Fig. 2H), as a marker for oligodendrocyte progenitor cells, demonstrated little colocalization with fibronectin messenger RNA and protein, respectively. Finally, some fibronectin messenger RNA–expressing cells occurred in association with blood vessels and had the morphology and arrangement of endothelial cells (Fig. 2I, inset). Double labelling with antibodies against fibronectin and von

Willebrand factor, a marker for endothelial cells, showed that some fibronectin co-localized with oval-shaped von Willebrand factor-positive cells (Fig. 2I, inset). This indicated that endothelial cells may also produce cellular fibronectin, as suggested before by the localization of EIIIA-fibronectin (Fig. 1), and co-localization of IST9 with von Willebrand factor (data not shown). Hence, macrophages/microglia, astrocytes and endothelial cells, but not cells of the oligodendrocytes lineage, contribute to cellular fibronectin expression in demyelinated lesions.

Fibronectin assembles into aggregates in demyelinated multiple sclerosis lesions

Previous studies suggest the expression of fibronectin in chronically demyelinated multiple sclerosis lesions (Sobel and Mitchell., 1989; van Horssen *et al*., 2005, 2006; Satoh *et al*., 2009). However, these studies do not provide information on fibronectin levels, its origin or its form. We therefore biochemically characterized fibronectin expression in white matter brain homogenates of healthy subjects (control white matter, $n = 9$), (chronic) active multiple sclerosis lesions ($n = 8$) and chronic inactive multiple sclerosis lesions ($n = 9$). In chronic inactive lesions, fibronectin was expressed around blood vessels (Fig. 3D), whereas an increased number of smaller fibronectin deposits were present throughout (chronic) active multiple sclerosis lesions (Fig. 3B and C). However, in control white matter, obtained from subjects without clinical or pathological signs of neurological disease, fibronectin was scarcely detectable and limited to the vasculature (Fig. 3A). Western blot analysis under reducing conditions confirmed the increased fibronectin expression in multiple sclerosis lesions as compared with control white matter (Fig. 3E). Although control white matter showed a variation in fibronectin levels among individual subjects, the amount of fibronectin in white matter homogenates of active and inactive multiple sclerosis lesions was generally higher (Fig. 3F). Therefore, our data provide quantitative evidence of fibronectin accumulation in multiple sclerosis lesions. Analysis of fibronectin messenger RNA expression via reverse transcriptase–PCR revealed low levels (Supplementary Fig. 3) that do not seem to be in line with the increased fibronectin protein levels in multiple sclerosis lesions (Fig. 3B), but could well be explained by the chronic status of these lesions. Accordingly, fibronectin messenger RNA might have been initially upregulated at the onset of demyelination, but downregulated over time, whereas the protein has not been degraded and subjected to post-transcriptional and post-translational modification, which we examined next.

Fibronectin normally appears as a disulphide-bound dimer with subunits of 220–250 kDa, but can assemble into a complex network of fibrils of high molecular weight aggregates, which are insoluble in the detergent deoxycholate (Wierzbicka-Patynowski and Schwarzbauer, 2003; Mao and Schwarzbauer, 2005). Under non-reducing SDS-PAGE conditions, fibronectin aggregates remain either in the stacking gel or just penetrate the resolving gel in lower percentage SDS cells. To examine whether fibronectin aggregates in multiple sclerosis lesions, we performed detergent deoxycholate (in)solubility assays. High molecular weight fibronectin complexes were observed in the deoxycholate-insoluble fraction from homogenates of multiple sclerosis lesions, whereas fibronectin dimers were the main form in control white matter (Fig. 3G). This suggests that fibronectin aggregates are predominantly present in both active and inactive multiple sclerosis lesions, and hardly in control white matter. Given our previous findings that fibronectin perturbs myelin-like membrane formation (Buttery and ffrench-Constant, 1999; Maier *et al*., 2005; Siskova *et al*., 2006, 2009) and given that clearance of fibronectin in toxin-induced demyelination preceded remyelination (Fig. 1), the detection of fibronectin aggregates in chronically demyelinated multiple sclerosis lesions led us to hypothesize that they may contribute to remyelination failure. If this is the case, fibronectin would not aggregate and/or aggregation would not persist in toxin-induced demyelination.

Fibronectin aggregates predominantly in inflammation-induced demyelination

Deoxycholate (in)solubility assays followed by SDS-PAGE under non-reducing conditions revealed that fibronectin aggregation was minimal in toxin-lesioned tissues (Fig. 3H). Hence, fibronectin expression was transiently upregulated on toxin-induced demyelination, but does not extensively aggregate. A major difference between multiple sclerosis and toxin-induced lesions is the mechanism of demyelination. In multiple sclerosis, demyelination results mainly from activity of the adaptive immune system, whereas in toxin-induced models, demyelination is caused by the toxin and this initiates a secondary inflammatory response, mainly involving the innate immune system. To assess whether fibronectin aggregation is mediated by chronic inflammation, we next examined fibronectin expression and aggregation in chronic relapsing EAE, an animal model of immune-mediated demyelination that resembles many clinical and pathological features of relapsing-remitting multiple sclerosis (Furlan *et al*., 2009; Pachner, 2011). On immunization with a myelin oligodendrocyte glycoprotein peptide, the animals suffer from neurological symptoms, usually restricted to the hind body, that develop in a relapsing-remitting pattern (Supplementary Fig. 4A). During the relapse phase, Major Histocompatibility Complex class II inflammatory infiltrates can be observed in the rat spinal cord (Supplementary Fig. 4B), whereas demyelinated areas can be observed in the lumbar and sacral region of the spinal cord (Storch *et al*., 1998; Ledeboer *et al*., 2003). Total fibronectin expression was increased at the relapse phase in chronic relapsing EAE by ~9-fold (Fig. 3I) compared with incomplete Freund's adjuvant control. Furthermore, deoxycholate-(in)solubility assays showed that fibronectin aggregated in chronic relapsing EAE (Fig. 3J), similar to multiple sclerosis lesions (Fig. 3B). EIIIA-fibronectin expression was also evident at the relapse in chronic relapsing EAE (Fig. 3K), suggesting that cellular fibronectin was increased as an immediate response on inflammation-mediated demyelination. Hence, whereas fibronectin was transiently expressed and remained predominantly soluble in toxin-induced demyelination undergoing remyelination, fibronectin aggregates were formed in lesions of inflammation-induced demyelination, where remyelination often fails. Therefore, we

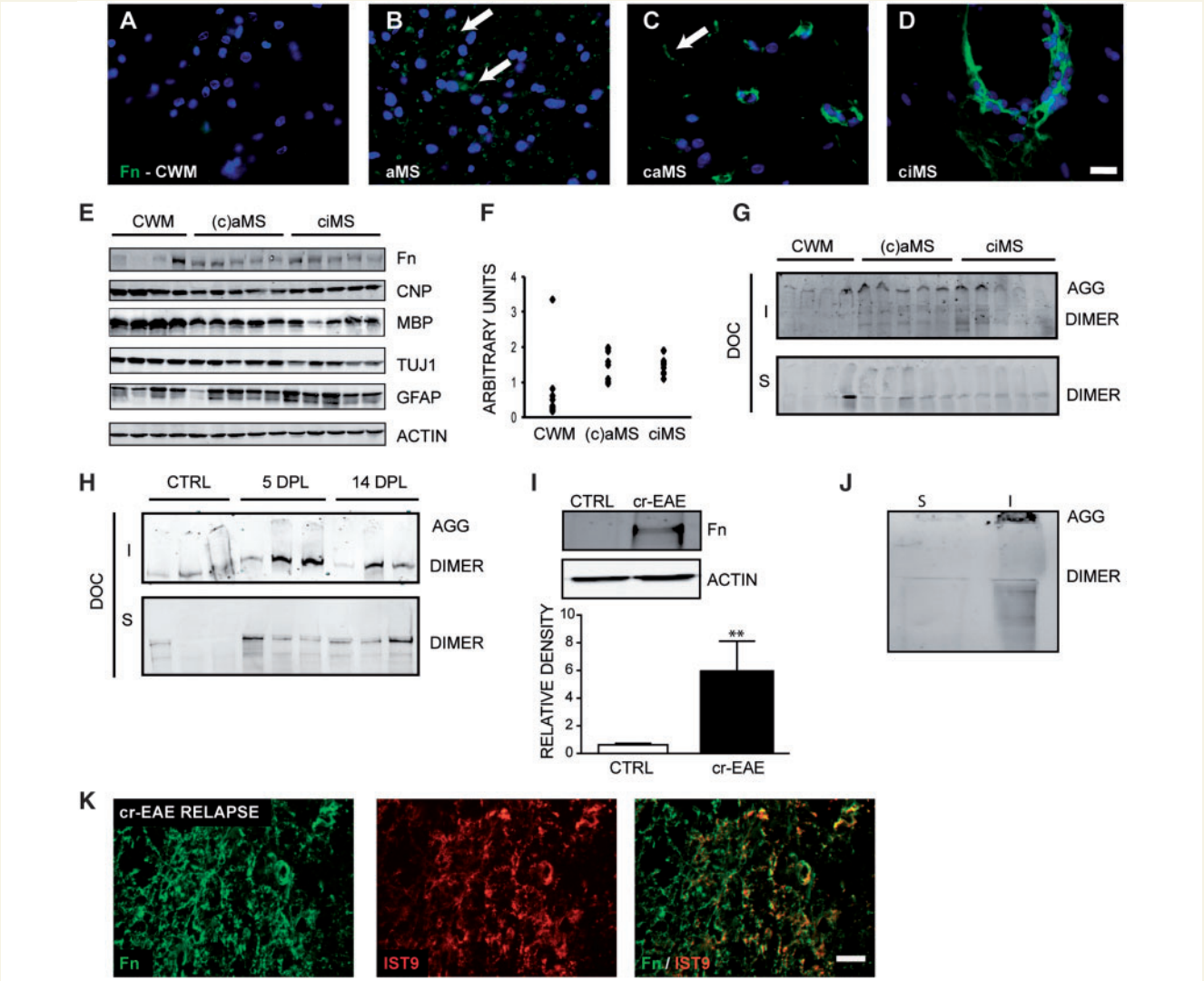

Figure 3 Fibronectin protein expression and biochemical characterization in human control white matter, multiple sclerosis lesions, chronic relapsing EAE and toxin-induced lesions. (**A–D**) Fibronectin expression (green) is abundant within the parenchyma of demyelinated multiple sclerosis lesion areas in active multiple sclerosis (**B**, arrows) and chronic active multiple sclerosis (arrow), and nearly absent from control white matter (CWM). In chronic inactive multiple sclerosis, fibronectin is abundantly expressed in association with blood vessels (**D**). Nuclei were counterstained with DAPI (blue). Representative images of control white matter (**A**) and centres of active (aMS, **B**), chronic active (caMS, **C**) and chronic inactive (ciMS, **D**) multiple sclerosis lesions are shown. Scale bar = 20 μm. (**E**) Expression levels of fibronectin and the other indicated proteins in 50 μg of brain white matter homogenates of human control white matter, (chronic) active and chronic inactive multiple sclerosis lesions as determined by western blot under reducing conditions (monomers). Demyelination of the lesions was confirmed by lower expression levels of the myelin protein MBP compared with control white matter. Decreased CNP levels, mostly in (chronic) active multiple sclerosis lesions, and decreased TuJ1-levels, particularly in chronic inactive lesions, were likely indicative of oligodendrocyte and axonal loss, respectively. The constant levels of actin in the samples served as internal controls. (**F**) Variation of fibronectin expression in individual human white matter tissue. (**G**) Fibronectin aggregates are abundantly present in (chronic) active multiple sclerosis and chronic inactive multiple sclerosis lesion homogenates compared with control white matter homogenates. Homogenates (100 μg) were subjected to deoxycholate-(in)solubility assays, and deoxycholate-insoluble (I) and -soluble (S) fractions were analysed by western blotting under non-reducing conditions. (**H**) Fibronectin aggregates are virtually absent from lysolecithin-induced demyelinated lesions. Deoxycholate-insoluble (I) and -soluble (S) fractions from 50 μg tissue were analysed by western blotting under non-reducing conditions. Three animals per condition were analysed. (**I**) Fibronectin expression is upregulated in chronic relapsing EAE animals as compared with incomplete Freund's adjuvant controls. Spinal cord homogenates (20 μg) of control (CTRL) and chronic relapsing EAE (cr-EAE, relapse phase) were analysed by western blotting under reducing conditions (monomers). Data were quantified by normalizing the optical densities of fibronectin protein against actin, and expressed as mean + SD (** $P < 0.01$ at Student's *t*-test, three animals per group). (**J**) Fibronectin aggregates at the relapse phase in chronic relapsing EAE. Deoxycholate-insoluble (I) and -soluble (S) fractions from 100 μg tissue were analysed by western blotting under non-reducing conditions. (**K**) Fibronectin (red) and EIIIA-fibronectin (IST9, green) expression at the relapse phase of chronic relapsing EAE. Scale bar = 20 μm. EIIIA-fibronectin and fibronectin particularly co-localize (yellow) around blood vessels. Fn = fibronectin; AGG = aggregate; DPL = days post lesion.

next examined whether inflammatory mediators induce fibronectin aggregation *in vitro*.

Fibronectin aggregation by cultured astrocytes is induced by the inflammatory mediator lipopolysaccharide

Having identified multiple cellular sources *in vivo,* we first examined which of these cells express fibronectin messenger RNA and protein in (primary) monoculture *in vitro*. Only cultured astrocytes produced fibronectin messenger RNA and fibronectin protein in considerable amounts (Fig. 4A), which corroborate previous findings that astrocytes produce fibronectin (Price and Hynes, 1985; Liesi *et al*., 1986; Oh and Yong, 1996). However, fibronectin expression by the other cell types may occur in other, particular activation states. Water-lysis of the cultured astrocytes showed that untreated astrocytes deposited fibronectin in an evenly distributed diffuse pattern, whereas astrocytes exposed to the inflammatory mediator lipopolysaccharide deposited a more localized fibrillar fibronectin matrix (Fig. 4B, rat). Similar results were obtained when astrocytes were removed by EDTA-mediated detachment (data not shown). Notably, an increase in fibronectin messenger RNA and a slight increase in protein expression were observed in astrocytes treated with the inflammatory mediator lipopolysaccharide (Fig. 4A). Fibronectin aggregation also markedly increased after treatment with lipopolysaccharide in rat

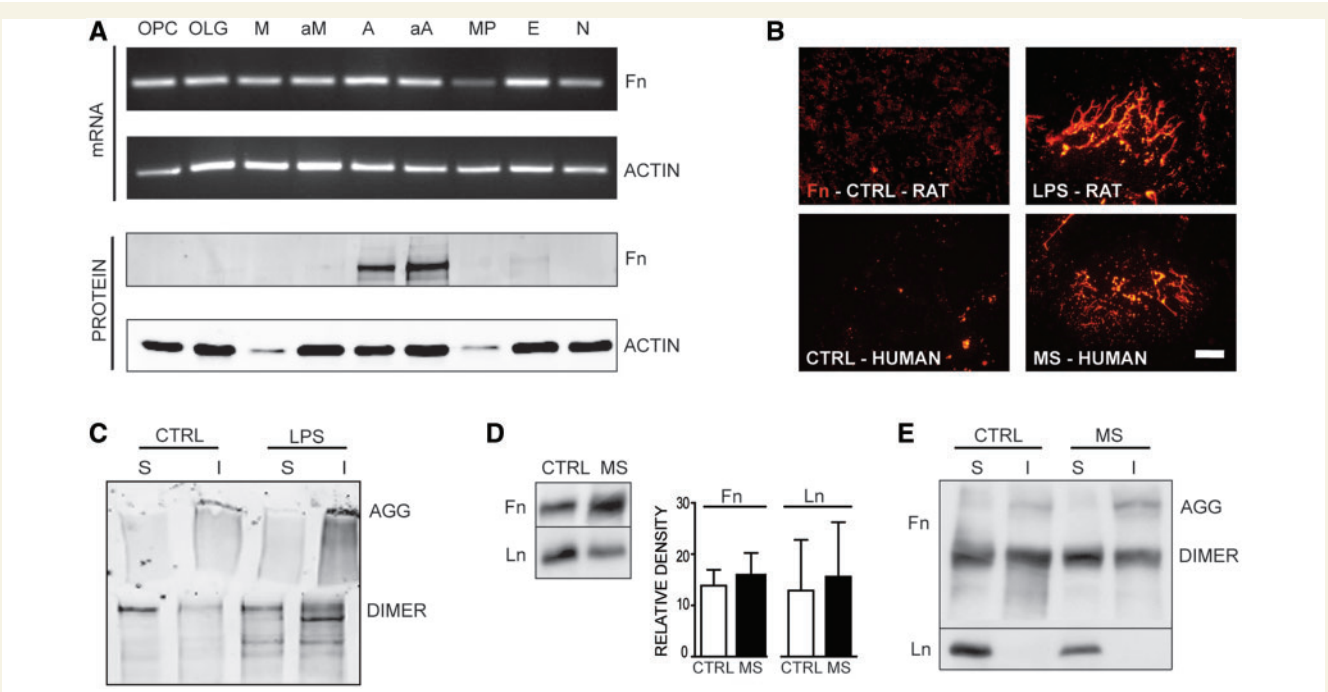

Figure 4 Fibronectin expression and aggregation in cultured cells. (**A**) Cultured astrocytes synthesize fibronectin protein in abundant levels. Primary rat oligodendrocyte progenitors (OPC), mature rat oligodendrocytes (OLG), rat microglia (M), rat lipopolysaccharide-activated microglia (aM), rat astrocytes (A), rat lipopolysaccharide-activated astrocytes (aA), bone-marrow derived macrophages (MP), rat cortical neurons (N) (de Jong *et al*., 2005) and the human brain endothelial cell line hCEMC/D3 (E) (Weksler *et al*., 2005) were analysed for fibronectin messenger RNA and protein expression using reverse transcriptase–PCR and western blot analysis (reducing conditions, monomers). A representative blot of three independent experiments is shown. (**B**) Astroglial matrices from both lipopolysaccharide-activated rat astrocytes (LPS) and human multiple sclerosis astrocytes (MS) contained fibrillar fibronectin structures, whereas control astrocytes (CTRL) showed a more diffuse deposition of fibronectin. Cultured astrocytes were water-lysed and remaining deposits were analysed for fibronectin deposition by immunofluorescence. Scale bar = 20 μm. Representative images of three to four independent experiments are shown. (**C**) Fibronectin aggregates are present in the matrix of lipopolysaccharide-stimulated (LPS), but not in the matrix of non-stimulated (CTRL) rat astrocytes. Deposits (10 μg) were subjected to deoxycholate-(in)solubility assays, and deoxycholate-insoluble (I) and -soluble (S) fractions were analysed by western blotting under non-reducing conditions. Representative blots and images of three to four independent experiments are shown. (**D**) Fibronectin and laminin (Ln) are expressed by cultured human astrocytes from healthy subjects (CTRL) and patients with multiple sclerosis (MS). Total cell lysates (10 μg) were analysed for fibronectin and laminin expression by western blotting under reducing conditions (monomers). Data were quantified by normalizing the optical densities of fibronectin and laminin protein against actin, and expressed as mean + SD ($P > 0.05$ at Student's *t*-test). (**E**) Presence of fibronectin aggregates is increased in the deoxycholate-insoluble fraction of multiple sclerosis astrocytes (MS) compared with normal astrocytes (CTRL), whereas laminin is deoxycholate soluble. Deposits (10 μg) were subjected to deoxycholate-(in)solubility assays, and deoxycholate-insoluble (I) and -soluble (S) fractions were analysed by western blotting under non-reducing conditions. Representative blots of the deposits of astrocyte cultures analysed in **D** are shown. Fn = fibronectin; AGG = aggregate.

astrocyte-derived matrices, as detected by deoxycholate-(in)solubility assays (Fig. 4C). Likewise, cultured human astrocytes isolated from patients with multiple sclerosis displayed the ability to deposit and to arrange fibronectin in fibrillar networks, whereas human astrocytes from healthy subjects deposited fibronectin in smaller more diffuse structures (Fig. 4B, human). In addition, astrocytes from multiple sclerosis tissue synthesized slightly more fibronectin and similar levels of laminin, which is a myelination permissive extracellular matrix molecule (Buttery and ffrench-Constant, 1999; Colognato *et al*., 2005; Siskova *et al*., 2006) compared with astrocytes from healthy subjects (Fig. 4D). Furthermore, multiple sclerosis astroglial matrices, but not those from healthy astrocytes, showed a clear band at the position of aggregated fibronectin in the deoxycholate-insoluble fraction (Fig. 4E), whereas deposited laminin appeared in the deoxycholate-soluble fraction (Fig. 4E). Also, preliminary proteomic analysis demonstrated that the deoxycholate-insoluble fraction mainly consists of fibronectin, i.e. ~10% of total protein, and does not contain other extracellular matrix proteins, such as hyaluronan and proteoglycans. These findings demonstrate that, although cultured astrocytes synthesize and deposit fibronectin, they do not induce aggregation unless additional factors, such as those linked to chronic inflammation, are present. This could explain why fibronectin aggregates were found at the relapse phase in chronic relapsing EAE and multiple sclerosis lesions, but not in toxin-induced demyelination. Because fibronectin aggregates in multiple sclerosis lesions, where remyelination fails, and not in toxin-induced lesions, where remyelination is complete, we next examined whether fibronectin aggregates contribute directly to remyelination failure.

Astrocyte-derived fibronectin aggregates inhibit remyelination

We first studied whether astrocyte-derived fibronectin aggregates altered progression within the oligodendrocytes lineage *in vitro*. To allow investigation of cell–matrix interactions as such, oligodendrocyte progenitor cells were plated onto astroglial matrices obtained from untreated (Fig. 4B) or lipopolysaccharide-treated rat astrocytes (Fig. 4B). The astrocytes were removed by water-lysis, so that the effect of live astrocytes and their soluble factors on oligodendrocyte progenitor cells was eliminated. When oligodendrocyte progenitor cells were cultured on the astrocyte-derived matrices for 7 days, a small increase in the number of MBP-positive cells, indicative for differentiation, was observed (Fig. 5A and B). Myelin-like membrane formation, as defined by cells bearing MBP-positive membranous structures spread between the cellular processes, however, was prevented on astroglial matrices from lipopolysaccharide-stimulated astrocytes, i.e. containing fibronectin aggregates, compared with oligodendrocyte progenitor cells cultured on astroglial matrices from untreated rat astrocytes (Fig. 5A and B). To further examine whether fibronectin aggregates in the total astroglial matrix indeed impair remyelination *in vivo*, enriched fibronectin aggregates, obtained from the deoxycholate-insoluble fraction of deposits from cultured rat astrocytes, were intralesionally injected in lysolecithin-induced demyelinated lesions at 7 days post lesion. Following fibronectin aggregate injection, the density of cells expressing the oligodendrocytes marker Olig2 seemed slightly reduced at 14 days post lesion, i.e. 7 days post aggregate injection, compared with saline-injected lesions (Fig. 5C and D), though not statistically significant. Notably, in saline-injected lesions, substantial fibronectin staining was still present, which is likely due to the response of fresh trauma by the (second) injection, although to a much lesser extent comparing with fibronectin aggregate–injected lesions (Supplementary Fig. 5A and B). The number of cells expressing the oligodendrocyte progenitor cell marker Nkx2.2 in the lesions was also not altered by fibronectin aggregates (Fig. 5E and F). Cells expressing oligodendrocyte differentiation markers APC protein (CC1) and proteolipid protein messenger RNA were, however, significantly decreased (Fig. 5G–J). Electron microscopy analysis at 14 days post lesion revealed that remyelination was impaired on fibronectin aggregate injection (Fig. 5K), which was reflected by a significant increase in the g-ratios ($P < 0.05$, Fig. 5L). To examine whether the reduction of mature oligodendrocytes was due to direct toxicity of fibronectin aggregates, the viability of oligodendrocyte cell lineage cells was assessed *in vitro* with a lactate dehydrogenase and MTT assay. Oligodendrocyte viability was not affected by addition of fibronectin aggregates to different maturation stages (Supplementary Fig. 5C and D), indicating that fibronectin aggregates are apparently not toxic to cultured oligodendrocytes. Therefore, these data indicate that astrocyte-derived fibronectin aggregates predominantly perturbed oligodendrocytes differentiation *in vivo* and impaired remyelination. These findings would imply that fibronectin aggregates must be absent from remyelinated multiple sclerosis lesions, i.e. shadow plaques, which were examined next.

Fibronectin aggregates are present at low level in remyelinated multiple sclerosis lesions

To assess whether fibronectin aggregates are expressed at remyelinating conditions, homogenates of remyelinated multiple sclerosis shadow plaque containing brain tissue were subjected to deoxycholate-(in)solubility assays. The status of shadow plaques was confirmed by the Netherlands Brain Bank, showing a slightly reduced expression of proteolipid protein compared with the surrounding normal-appearing white matter, without abundant expression of CD68. Fibronectin aggregates were weakly expressed in the examined multiple sclerosis shadow plaques, whereas fibronectin is mainly present as a deoxycholate-soluble dimer (Fig. 6A). Furthermore, western blot analysis at reducing conditions revealed that fibronectin levels are slightly increased in remyelinated multiple sclerosis lesions compared with control white matter, but to a lesser extent than in (chronic) active multiple sclerosis lesions (Fig. 6B). Fibronectin staining around blood vessels can be discerned throughout the shadow plaques (Fig. 6C), and seemed higher than fibronectin staining in surrounding normal-appearing white matter (data not shown). However, fibronectin is barely detectable in the parenchyma of the remyelinated area. Thus, fibronectin aggregates are present at a low level in

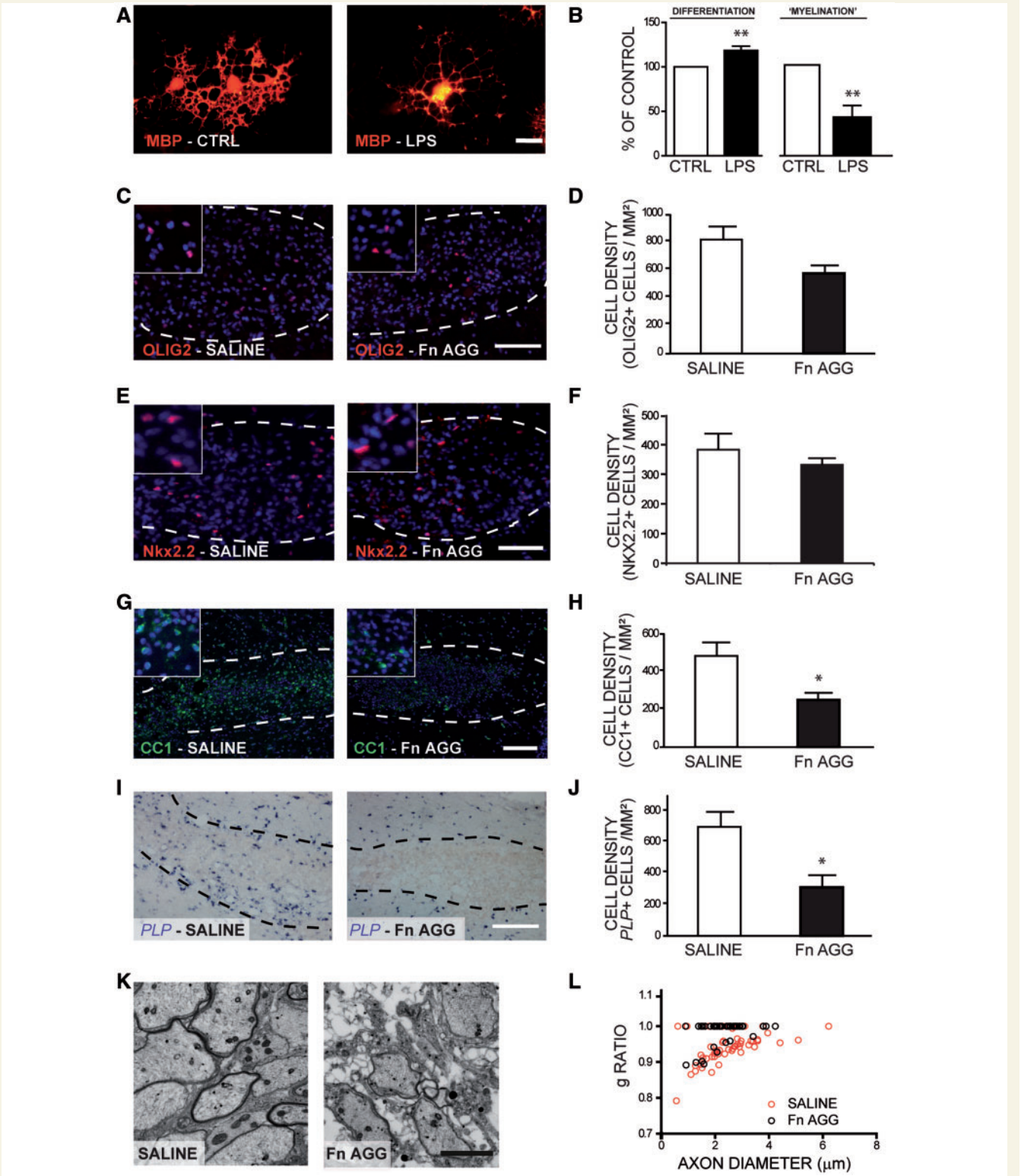

Figure 5 Effects of fibronectin aggregates on oligodendrocytes *in vitro* and *in vivo*. (**A** and **B**) Oligodendrocyte progenitor cells differentiate to MBP-expressing oligodendrocytes on control (CTRL) and fibronectin aggregate (LPS) containing astroglial extracellular matrices, but myelin-like membrane formation was retarded on fibronectin aggregates. This is confirmed by quantification of MBP-positive cells (**B**, differentiation) and the amount of MBP-positive cells elaborating myelin-like membranes (**B**, myelination). Astroglial matrices were obtained by water-lysis of astrocytes. In each experiment, at least 500 cells/well were counted. To compare different independent experiments, the data are expressed as per cent of control, i.e. values obtained from CTRL were set to 100. Each bar represents the mean + SEM of three independent experiments. Statistical differences were assessed with a Student's *t*-test, and are indicated by asterisks ($*P < 0.05$, $**P < 0.01$). Representative images of three independent experiments are shown (**A**). Scale bar = 20 μm. (**C**–**L**) Fibronectin

(continued)

remyelinated multiple sclerosis lesions, which corroborate the findings that fibronectin aggregates impair remyelination.

Discussion

Remyelination is crucial for functional recovery in demyelinating diseases, such as multiple sclerosis (Duncan *et al*., 2009). Here, we show that the extracellular matrix component fibronectin, which is largely absent from healthy adult white matter, rapidly accumulates as an acute response to demyelination, but disappears on remyelination. However, in multiple sclerosis lesions where remyelination fails, a persistent accumulation of stable aggregated fibronectin occurs. These fibronectin aggregates are most likely generated by astrocytes on engagement with inflammatory mediators, and most relevantly, these aggregates impair remyelination.

Aggregation of fibronectin is likely associated with the process of inflammation. This was suggested by the absence of fibronectin aggregates from toxin-induced demyelination, where an innate immune response is secondary to demyelination, compared with the abundance of fibronectin aggregates in chronic relapsing EAE and multiple sclerosis lesions, where demyelination is caused by the adaptive immune response. Also, our *in vitro* experiments with primary rat astrocytes suggest a role for inflammatory mediators in fibronectin aggregation. Astrocytes exposed to the inflammatory mediator lipopolysaccharide deposit fibronectin in fibril-like structures, whereas untreated astrocytes deposit fibronectin in a more diffuse pattern. This structural difference in fibronectin appearance is monitored by conversion from a deoxycholate-soluble dimeric form to deoxycholate-insoluble fibronectin aggregates. Fibrillar fibronectin assembly is primarily initiated by binding of soluble fibronectin dimers to integrin $\alpha5\beta1$, followed by assembly into high molecular weight fibronectin that is cross-linked by non-covalent bounds (Wu *et al*., 1993, 1995; Wierzbicka-Patynowski and Schwarzbauer, 2003; Ohashi and Erickson, 2009). Integrin $\alpha5\beta1$ is expressed on astrocytes (King *et al*., 2001), neurons (King *et al*., 2001) and activated microglia (Milner *et al*., 2007), but not on oligodendrocytes (Milner and ffrench-Constant, 1994). In addition to fibril formation, fibronectin can be covalently cross-linked by enzymes. Tumor necrosis

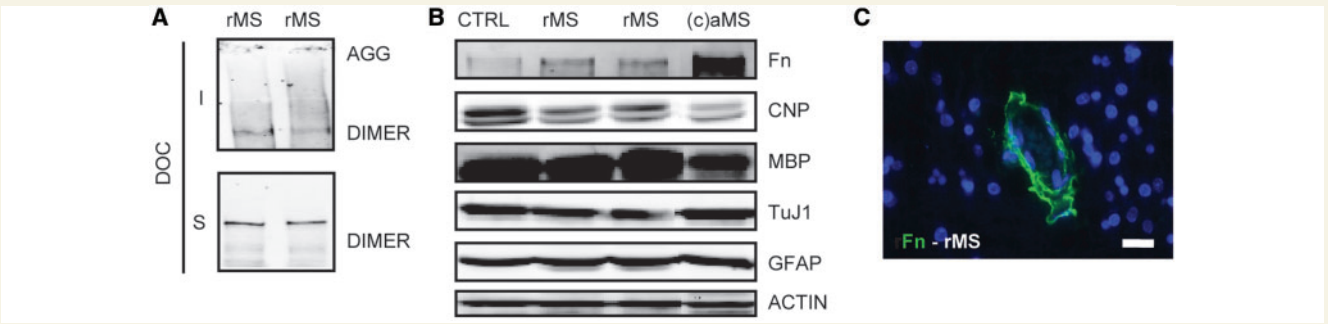

Figure 6 Fibronectin protein expression and biochemical characterization in remyelinated multiple sclerosis lesions. (**A**) Expression levels of fibronectin aggregates and dimers in remyelinated multiple sclerosis lesions. Homogenates (100 μg) were subjected to deoxycholate-(in)solubility assays, and deoxycholate-insoluble (I) and -soluble (S) fractions were analysed by western blotting under non-reducing conditions. (**B**) Total fibronectin expression in remyelinated multiple sclerosis lesions, compared with control white matter (CWM), and (chronic) active multiple sclerosis lesions. [(c)aMS]. Expression levels of fibronectin and the other indicated proteins were detected by subjecting 50 μg of human brain white matter homogenates to western blot analysis under reducing conditions. (**C**) Immunohistochemistry for fibronectin in multiple sclerosis shadow plaque lesions, where fibronectin was detected in a shape typical for blood vessels. A representative image of two different remyelinated lesions is shown. Scale bar is 20 μm. rMS = remyelinated multiple sclerosis shadow plaque; Fn = fibronectin; AGG = aggregate.

Figure 5 Continued

aggregates impair oligodendrocytes differentiation and remyelination *in vivo*. Deoxycholate-insoluble fibronectin aggregates (Fn AGG) obtained from rat astrocyte-derived deposits were intralesionally injected into demyelinated lesions of rats, 7 days after lysolecithin-induced demyelination, and then analysed at 14 days post lesion, i.e. 7 days post injection. (**C–J**) Images in **C**, **E**, **G** and **I** are representative images of demyelinated areas on saline (*left*) and fibronectin aggregate injection. The outline of the lesions was measured using AxoVision software on the basis of the increase in DAPI staining. The numbers of Olig2 (**C**), Nkx2.2 (**E**), CC1 (**G**) or proteolipid protein messenger RNA (PLP, **I**) positive cells were manually counted three times. There are three to four animals per group and three lesions per animal at a distance of ~120 μM apart from each other were analysed. The quantifications are shown in **D**, **F**, **H** and **J**, respectively. Each bar represents the mean + SEM. Statistical differences were assessed with a Student's *t*-test, and are indicated by asterisks (*$P < 0.05$). Scale bar = 100 μm. (**K** and **L**) Images are representative electromicrographs of demyelinated areas on saline (*left*) and fibronectin aggregate injection. The *g*-ratio of individual axons from saline injected (red circles) and fibronectin aggregate (black circles) were plotted against the corresponding axon diameters. The average *g*-ratio in fibronectin aggregated injected demyelinated areas is significantly higher than on saline injection ($P < 0.05$, Student's *t*-test, three animals per group). Scale bar in **K** = 2 μm.

factor-α, for example, increases fibronectin aggregation in endothelial cell layers by an enhanced transglutaminase activity on their surface (Chen *et al*., 2000), a process that might be active in multiple sclerosis lesions (van Strien *et al*., 2011). Hence, both persistent and recurring inflammation as well as concomitant astrogliosis could gradually result in conformation and accumulation of aggregated fibronectin in multiple sclerosis lesions.

Fibronectin expression in multiple sclerosis lesions was previously suggested to result from blood–brain barrier disruption (Sobel and Mitchell., 1989; van Horssen *et al*., 2005). Our data reveal that on CNS injury, CNS resident cells also contribute to the fibronectin pool. This conclusion is supported by at least three observations: (i) next to a typical vasculature localization, small fibronectin deposits are present in multiple sclerosis, chronic relapsing EAE and toxin-induced lesions, suggesting additional sources to plasma leakage; (ii) fibronectin messenger RNA is upregulated in toxin-induced demyelination; and (iii) EIIIA-fibronectin protein is detected at the lesion site. The lack of fibronectin messenger RNA, likely due to the chronic disease status, precluded elucidation of cellular sources in multiple sclerosis lesions. However, *in situ* hybridization co-localization studies in toxin-induced lesion revealed that astrocytes, microglia/macrophages and endothelial cells likely synthesize fibronectin. Whether these cells also secrete and actively deposit fibronectin *in vivo* is rather difficult to determine. *In vitro*, fibronectin aggregation is dependent on astrocytes, as only astrocytes actively synthesize and deposit fibronectin, and plasma fibronectin alone, i.e. in the absence of astrocytes, does not aggregate (our unpublished observations). However, plasma fibronectin likely incorporates into astrocyte-derived fibronectin aggregates (McKeown-Longo and Mosher, 1983; Peters *et al*., 1990).

Importantly, our data revealed that aggregated fibronectin impairs remyelination. Fibronectin aggregates are hardly present in remyelinated multiple sclerosis shadow plaques, and injection of astrocyte-derived fibronectin aggregates into lysolecithin-induced demyelinated lesions resulted in a significant decrease of differentiated oligodendrocytes and concomitant increase in g-ratio compared with saline-injected lesions. Myelin-like membrane formation *in vitro* is inhibited by astrocyte-derived matrix that contains fibronectin aggregates, but not by astrocyte-derived matrix that contains dimeric fibronectin. This might be explained by the presence of additional (extracellular matrix) molecules that reside in the total astroglial matrix, such as laminin (Liesi *et al*., 1983, 1984; Fig. 4D and E). These additional molecules could overcome the myelination-inhibiting effect of dimeric fibronectin that has been observed previously (Buttery and ffrench-Constant, 1999; Maier *et al*., 2005; Siskova *et al*., 2006, 2009). Indeed, laminin signals are known to dominate over dimeric plasma fibronectin inhibitory signals (Buttery and ffrench-Constant, 1999). The presence of additional proteins in total astrocyte deposits may therefore also explain why fibronectin aggregates affect oligodendrocyte differentiation only *in vivo,* as the intralesionally injected aggregates were deoxycholate-insoluble, therefore lacking laminin and other glycoproteins (Fig. 4D and E). The inhibitory effect of fibronectin aggregates may occur through different mechanisms. First, fibronectin aggregates could directly affect oligodendrocyte progenitor cells through the classical fibronectin receptors, αv integrins, which they upregulate in toxin-induced lesions (Zhao *et al*., 2009). Alternatively, the interaction of aggregates with other cell types *in vivo* might indirectly affect oligodendrocyte differentiation and remyelination. Finally, fibronectin aggregation likely involves biochemical restructuring of fibronectin (Johnson *et al*., 1999; Baneyx *et al*., 2002), which could expose different conformation-dependent binding sites that provoke altered signalling properties (Morla *et al*., 1994; Pasqualini *et al*., 1996; Sottile *et al*., 1998).

In conclusion, myelin regeneration following demyelination is a dynamic process, and requires a spatial and timely balanced response of the extracellular microenvironment. Temporal dimeric fibronectin expression by astrocytes might be important in regulating remyelination at earlier stages. Pathological fibronectin aggregates as observed in multiple sclerosis lesions do, however, likely contribute to remyelination failure. Therefore, strategies to promote remyelination should not aim at preventing fibronectin deposition, but at interfering with fibronectin aggregation and clearance. In addition, the effects of persistent fibronectin aggregates on other CNS cells, including microglia and neurons, as well as the mechanisms of how aggregation is mediated, warrant further investigation, particularly because protein aggregation is likely central to the pathology of several other neurodegenerative diseases (Jucker and Walker, 2011).

Acknowledgements

We thank the Netherlands Brain Bank for providing autopsy tissue, Dr. Malika Bsibsi (Delta Crystallon BV, Leiden, the Netherlands) for providing us with human astrocytes and Sonja van der Veen and Dr. Erik Sikkema for expert technical assistance.

Funding

This work was supported by grants from the Dutch MS Research Foundation (‘Stichting MS Research’, W.B., J.M.J.S.), the UK MS Society (C.Z., R.J.M.F.), the Netherlands Organization of Scientific Research [NWO, W.B. (VIDI and Aspasia), Z.S.], Prinses Beatrix Fonds (J.M.J.S.), Marco Polo Fonds (J.M.J.S.), J.K. de Cock Stichting (J.M.J.S.), and Groninger Universiteits Fonds (J.M.J.S.).

Supplementary material

Supplementary material is available at *Brain* online.

References

Back SA, Tuohy TM, Chen H, Wallingford N, Craig A, Struve J, et al. Hyaluronan accumulates in demyelinated lesions and inhibits oligodendrocyte progenitor maturation. Nat Med 2005; 11: 966–72.

Baneyx G, Baugh L, Vogel V. Fibronectin extension and unfolding within cell matrix fibrils controlled by cytoskeletal tension. Proc Natl Acad Sci USA 2002; 99: 5139–43.

Baron W, Colognato H, ffrench-Constant C. Integrin-growth factor interactions as regulators of oligodendroglial development and function. Glia 2005; 49: 467–79.

Baron W, Decker L, Colognato H, ffrench-Constant C. Regulation of integrin growth factor interactions in oligodendrocytes by lipid raft microdomains. Curr Biol 2003; 13: 151–5.

Blakemore WF, Franklin RJM. Remyelination in experimental models of toxin-induced demyelination. Curr Top Microbiol Immunol 2008; 318: 193–212.

Bsibsi M, Nomden A, van Noort JM, Baron W. Toll-like receptors 2 and 3 agonists differentially affect oligodendrocyte survival, differentiation, and myelin membrane formation. J Neurosci Res 2012; 90: 388–98.

Bsibsi M, Ravid R, Gveric D, van Noort JM. Broad expression of Toll-like receptors in the human central nervous system. J Neuropathol Exp Neurol 2002; 61: 1013–21.

Buttery PC, ffrench-Constant C. Laminin-2/integrin interactions enhance myelin membrane formation by oligodendrocytes. Mol Cell Neurosci 1999; 3: 199–212.

Chari DM, Zhao C, Kotter MR, Blakemore WF, Franklin RJ. Corticosteroids delay remyelination of experimental demyelination in the rodent central nervous system. J Neurosci Res 2006; 83: 594–605.

Chen R, Gao B, Huang C, Olsen B, Rotundo RF, Blumenstock F, et al. Transglutaminase-mediated fibronectin multimerization in lung endothelial matrix in response to TNF-α. Am J Physiol Lung Cell Mol Physiol 2000; 27: L161–74.

Colognato H, Baron W, Avellana-Adalid V, Relvas JB, Baron-Van Evercooren A, Georges-Labouesse E, et al. CNS integrins switch growth factor signalling to promote target-dependent survival. Nat Cell Biol 2002; 4: 833–41.

Colognato H, ffrench-Constant C, Feltri ML. Human diseases reveal novel roles for neural laminins. Trends Neurosci 2005; 28: 480–86.

de Jong EK, Dijkstra IM, Hensens M, Brouwer N, van Amerongen M, Liem RS, et al. Vesicle-mediated transport and release of CCL21 in endangered neurons: a possible explanation for microglia activation remote from a primary lesion. J Neurosci 2005; 17: 7548–57.

Duncan ID, Brower A, Kondo Y, Curlee JF Jr, Schultz RD. Extensive remyelination of the CNS leads to functional recovery. Proc Natl Acad Sci USA 2009; 106: 6832–6.

Fancy SPJ, Zhao C, Franklin RJM. Increased expression of Nkx2.2 and Olig2 identifies reactive oligodendrocyte precursor cells responding to demyelination in the adult CNS. Mol Cell Neurosci 2004; 27: 247–54.

Franklin RJ, ffrench-Constant C. Remyelination in the CNS: from biology to therapy. Nat Rev Neurosci 2008; 9: 839–55.

Furlan R, Cuomo C, Martino G. Animal models of multiple sclerosis. Methods Mol Biol 2009; 549: 157–73.

Goldschmidt T, Antel J, Konig FB, Bruck W, Kuhlmann T. Remyelination capacity of the MS brain decreases with disease chronicity. Neurology 2009; 72: 1914–21.

Gutowski NJ, Newcombe J, Cuzner ML. Tenascin-R and C in multiple sclerosis lesions: relevance to extracellular matrix remodelling. Neuropathol Appl Neurobiol 1999; 25: 207–14.

Johnson KJ, Sage H, Briscoe G, Erickson HP. The compact conformation of fibronectin is determined by intramolecular ionic interactions. J Biol Chem 1999; 274: 15473–9.

Jucker M, Walker LC. Pathogenic protein seeding in Alzheimer disease and other neurodegenerative disorders. Ann Neurol 2011; 70: 532–40.

King VR, McBride A, Priestley JV. Immunohistochemical expression of the alpha5 integrin subunit in the normal adult rat central nervous system. J Neurocytol 2001; 30: 243–52.

Kuhlmann T, Miron V, Cuo Q, Wegner C, Antel J, Bruck W. Differentiation block of oligodendroglial progenitor cells as a cause for remyelination failure in chronic multiple sclerosis. Brain 2008; 131: 1749–58.

Ledeboer A, Wierinckx A, Bol J, Floris S, Renardel de Lavalette C, De Vries HE, et al. Regional and temporal expression patterns of interleukin-10, interleukin-10 receptor and adhesion molecules in the rat spinal cord during chronic relapsing EAE. J Neuroimmunol 2003; 136: 94–103.

Lee MK, Tuttle JB, Rebhun LI, Cleveland DW, Frankfurter A. The expression and posttranslational modification of a neuron-specific beta-tubulin isotype during chick embryogenesis. Cell Motil Cytoskeleton 1999; 17: 118–32.

Liesi P, Dahl D, Vaheri A. Laminin is produced by early rat astrocytes in primary culture. J Cell Biol 1983; 96: 920–4.

Liesi P, Kaakkola S, Dahl D, Vaheri A. Laminin is induced in astrocytes of adult brain by injury. EMBO J 1984; 3: 683–6.

Liesi P, Kirkwood T, Vaheri A. Fibronectin is expressed by astrocytes cultured from embryonic and early postnatal brain. Exp Cell Res 1986; 163: 175–85.

Maier O, Baron W, Hoekstra D. Reduced raft-association of NF155 in active MS-lesions is accompanied by the disruption of the paranodal junction. Glia 2007; 55: 885–95.

Maier O, van der Heide T, van Dam AM, Baron W, de Vries H, Hoekstra D. Alteration of the extracellular matrix interferes with raft association of neurofascin in oligodendrocytes. Potential significance for multiple sclerosis? Mol Cell Neurosci 2005; 28: 390–401.

Mao Y, Schwarzbauer JE. Fibronectin fibrillogenesis, a cell-mediated matrix assembly process. Matrix Biol 2005; 24: 389–99.

McKeown-Longo PJ, Mosher DF. Binding of plasma fibronectin to cell layers of human skin fibroblasts. J Cell Biol 1983; 100: 364–74.

Milner R, Crocker SJ, Hung S, Wang X, Frausto RF, del Zoppo GJ. Fibronectin- and vitronectin-induced microglial activation and matrix metalloproteinase-9 expression is mediated by integrins α5β1 and αvβ5. J Immunol 2007; 178: 8158–67.

Milner R, ffrench-Constant C. A developmental analysis of oligodendroglial integrins in primary cells: changes in alpha v-associated beta subunits during differentiation. Development 1994; 120: 3497–506.

Morla A, Zhang Z, Ruoslathi E. Superfibronectin is a functionally distinct form of fibronectin. Nature 1994; 367: 193–6.

Oh LY, Yong VW. Astrocytes promote process outgrowth by adult human oligodendrocytes in vitro through interaction between FGF and astrocyte extracellular matrix. Glia 1996; 17: 237–53.

Ohashi T, Erickson HP. Revisiting the mystery of fibronectin multimers: the fibronectin matrix is composed of fibronectin dimers cross-linked by non-covalent bounds. Matrix Biol 2009; 28: 170–5.

Pachner AR. Experimental models of multiple sclerosis. Curr Opin Neurol 2011; 24: 291–9.

Pasqualini R, Bourdoulous S, Koivunen E, Woods VL, Ruoslathi E. A polymeric form of fibronectin with monoclonal antibodies and proteolytic fragments of the molecule. Nat Med 1996; 2: 1197–203.

Peters DM, Portz LM, Fullenwider J, Mosher DF. Co-assembly of plasma and cellular fibronectins into fibrils in human fibroblast cultures. J Cell Biol 1990; 111: 249–56.

Price J, Hynes RO. Astrocytes in culture synthesize and secrete a variant form of fibronectin. J Neurosci 1985; 5: 2205–11.

Relvas JB, Setzu A, Baron W, Buttery PC, LaFlamme SE, Franklin RJ, et al. Expression of dominant-negative and chimeric subunits reveals an essential role for beta1 integrin during myelination. Curr Biol 2001; 11: 1039–43.

Satoh JI, Tabunoki H, Yamamura T. Molecular network of the comprehensive multiple sclerosis brain-lesion proteome. Mult Scler 2009; 15: 531–41.

Scanzello CR, Plaas A, Crow MK. Innate immune system activation in osteoarthritis: is osteoarthritis a chronic wound? Curr Opin Rheumatol 2008; 20: 565–72.

Sim FJ, Hinks GL, Franklin RJ. The re-expression of the homeodomain transcription factor Gtx during remyelination of experimentally induced demyelinating lesions in young and old rat brain. Neuroscience 2000; 100: 131–9.

Siskova Z, Baron W, Vries de H, Hoekstra D. Fibronectin impedes 'myelin sheet' directed flow in oligodendrocytes: a role for the beta 1 integrin mediated PKC signaling in vesicular trafficking. Mol Cell Neurosci 2006; 33: 150–9.

Siskova Z, Yong VW, Nomden A, van Strien M, Hoekstra D, Baron W. Fibronectin attenuates process outgrowth in oligodendrocytes by mislocalizing MMP-9 activity. Mol Cell Neurosci 2009; 42: 234–42.

Sobel RA, Mitchell ME. Fibronectin in multiple sclerosis lesions. Am J Pathol 1989; 135: 161–8.

Sottile J, Hocking DC, Swiatek PJ. Fibronectin assembly enhances adhesion-dependent cell growth. J Cell Sci 1998; 111: 2933–43.

Stancic M, van Horssen J, Thijssen VL, Gabius HJ, van der Valk P, Hoekstra D, et al. Increased expression of distinct galectins in multiple sclerosis lesions. Neuropathol Appl Neurobiol 2011; 37: 654–71.

Storch MK, Stefferl A, Brehm U, Weissert R, Wallstrom E, Kerschensteiner M, et al. Autoimmunity to myelin oligodendrocyte glycoprotein in rats mimics the spectrum of multiple sclerosis pathology. Brain Pathol 1998; 8: 681–94.

Van Horssen J, Bö L, Dijkstra CD, de Vries HE. Extensive extracellular matrix depositions in active multiples sclerosis lesions. Neurobiol Dis 2006; 24: 484–91.

Van Horssen J, Bö L, Vos CM, Virtanen I, de Vries HE. Basement membrane proteins in multiple sclerosis-associated inflammatory cuffs: potential role in influx and transport of leukocytes. J Neuropathol Exp Neurol 2005; 64: 722–9.

Van Strien ME, Drukarch B, Bol JG, Van Der Valk P, Van Horssen J, Gerritsen WH, et al. Appearance of tissue transglutaminase in astrocytes in multiple sclerosis lesions: a role in cell adhesion and migration? Brain Pathol 2011; 21: 44–54.

Weksler BB, Subileau EA, Perrière N, Charneau P, Holloway K, Leveque M, et al. Blood-brain barrier-specific properties of a human adult brain endothelial cell line. FASEB J 2005; 19: 1872–4.

Wierzbicka-Patynowski I, Schwarzbauer JE. The ins and outs of fibronectin matrix assembly. J. Cell Sci 2003; 116: 3269–76.

Woodruff RH, Franklin RJ. Demyelination and remyelination of the caudal cerebellar peduncle of adult rats following a stereotaxic injections of lysolecithin, ethidium bromide, and complement/anti-galactocerebroside: a comparative study. Glia 1999; 25: 216–28.

Wu C, Bauer JS, Juliano RL, McDonald JA. The $\alpha 5\beta 1$ integrin fibronectin receptor, but not the $\alpha 5$ cytoplasmic domain, functions in an early and essential step in fibronectin matrix assembly. J Biol Chem 1993; 268: 21883–8.

Wu C, Keivens WM, O'Toole TE, MacDonald JA, Ginsberg MH. Integrin activation and cytoskeletal interaction are essential for the assembly of a fibronectin matrix. Cell 1995; 83: 715–24.

Zawadzka M, Rivers LE, Fancy SPJ, Zhao C, Tripathi R, Jamen F, et al. CNS-resident glial progenitor/stem cells produce Schwann cells as well as oligodendrocytes during repair of CNS demyelination. Cell Stem Cell 2010; 6: 578–90.

Zhao C, Fancy SP, ffrench-Constant C, Franklin RJ. Osteopontin is extensively expressed by macrophages following CNS demyelination but has a redunant role in remyelination. Neurobiol Dis 2008; 31: 209–17.

Zhao C, Fancy SP, Franklin RJM, ffrench-Constant C. Up-regulation of oligodendrocyte precursor cell αv integrin and its extracellular ligands during central nervous system remyelination. J Neurosci Res 2009; 87: 3447–55.

Zhao C, Li WW, Franklin RJ. Differences in the early inflammatory response to toxin-induced demyelination are associated with the age-related decline in CNS remyelination. Neurobiol Aging 2006; 27: 1298–1307.